Electronic Supplementary Material (ESI) for Materials Horizons.

Fluorescent Chemo-sensors Based on "Dually Smart" Optical Micro/nano-waveguides Lithographically Fabricated with AIE Composite Resins

Meng-Dan Qian[a], Yun-Lu Sun[b*], Zhi-Yong Hu[a], Xiao-Feng Fang[c], Jin-Long Zhu[d], Xudong Fan[b], Qing Liao[d], Chang-Feng Wu[c*], Hong-Bo Sun[e*]

[a]State Key Laboratory of Integrated Optoelectronics, College of Electronic Science and Engineering, Jilin University, 2699 Qianjin Street, Changchun 130012, China

[b]Department of Biomedical Engineering, University of Michigan, Ann Arbor, MI 48109, USA, E-mail: yunlus@umich.edu

[c]Department of Biomedical Engineering, Southern University of Science and Technology, Shenzhen, Guangdong 510855, China, E-mail: wucf@sustech.edu.cn

[d]Beijing Key Laboratory for Optical Materials and Photonic Devices, Department of Chemistry, Capital Normal University, Beijing 100048, China

[e]State Key Laboratory of Precision Measurement Technology and Instruments, Department of Precision Instrument, Tsinghua University, Beijing 100084, China, E-mail: hbsun@tsinghua.edu.cn

Experimental Section

Computational calculations of designed AIEoxes: The basic structures of AIEoxes are constructed via Gaussview 5.0 and the geometry optimization is performed with Gaussion 09 software. Related electronic structures and photophysical properties of designed AIEoxes are theoretically studied by the time-dependent density function theory (TD-DFT) method. The ground-state (S_0) geometry of AIEoxe is optimized using the functional B3LYP combined with 6-31G* basis sets in the solvent of chloroform via polymer continuum model (PCM). In this work, we simply choose the widely used B3LYP functional method for the computation, which may be not perfectly appropriate for the AIEoxe systems and result in small deviations to the experimental results. Even though the computed results are not very accurate, they generally conform with the experimental results, which help us to understand some photophysical information (e.g. absorbance spectra, electron cloud distribution, energy gap) from a theoretical perspective.

Preparation of AIEoxe composite resins and single-photon lithography: The AIEoxe molecules of three primary colors (i.e., red, green and blue) were purposely synthesized here (see details on the synthesis in our other study). The AIEoxes were firstly dissolved into THF to get a 200 mg/ml solution, which was uniformly mixed with commercial epoxy resin (SU8-2025, Microchem Corp.) with a mass ratio of 10% to obtain a composite resin for photolithography. Then, a 10-μm thick film was spin coated on as-need substrates (i.e., glass cover slices, low refractive-index glass or quartz slides). After spinning, the film was pre-baked under 40^{o}C in a vacuum drying oven for 8 hours prior to the lithography process. The large-area 2D micro-pattern arrays were generated by single-photon photolithography using a masker aligner ABM/6/350/NUV/DCCD/M (15 mW cm^{-2}, ABM Inc., American). The resin film was exposed for three seconds and experienced with a post-bake for 5 min at 90^{o}C, followed by the development in SU8 developer for 1 min to remove the unexposed parts.

FsLDLW fabrication of micro-patterns and waveguides: The waveguides were fabricated on the fused quartz plate with a low refractive index of ~1.4, so that the optical confinement and propagation along micro/nano-waveguides can be realized. The FsLDW system was self-built using a mode-locked Ti:Sapphire laser. The femtosecond laser beam with central wavelength of 800 nm and a pulse duration of 120 fs was focused by a 60× oil immersion objective lens (Olympus, numerical aperture (NA), 1.42). Laser power, scanning step length and single-point exposure time were optimized. The pre-bake was similar with that for above-mentioned single-photon lithography. After the post-bake at 90^{o}C for 15 min, the sample was immersed in the developer bath for 2 min to get the final micro-structures/devices. The specific structure design was aided with the computer towards flexible and facile on-demand manufacturing.

Characterizations: UV-vis absorption spectra were recorded by a Shimadzu UV-2550 spectrometer. The photoluminescence spectra and photostability curves of AIE and SU8-AIE film were measured by Hitachi F-4600 spectrophotometer. In the photostability assay, the fluorescence intensity of each composite film is monitored every 120 s under the consecutive irradiation of a 150 W xenon-lamp. The excitation slit width is set as 10 nm to allow for more excitation light and emission slit width is 1 nm. Fourier transform infrared (FTIR) spectra were collected from the Nicolet 6700 FTIR spectrometer. The morphology of fabricated micro-patterns is characterized by a field emission scanning electron microscope (Japan, JEOL JSM-6700F). Fluorescent images and the 3D surface profiles were measured using the laser confocal fluorescent microscope (Japan, OLS4100) equipped with 405 nm near-ultraviolet laser. The photoluminescence (PL) spectra and optical loss of waveguides were measured by a home-made optical microscope (objective, 50×, NA 0.9). The 400 nm laser beam from a semiconductor continuous-wave laser was focused on specific parts of the micro/nano-waveguides to excite fluorescence, which was recorded by a streak camera (C5680, Hamamatsu Photonics) with a polychromator (Chromex, Hamamatsu Photonics, spectral resolution, 0.2 nm).

The VOC sensing and photosbleaching assay of micro-structures: In the VOCs sensing process, typical water-soluble VOCs (i.e., EtOH, acetone, THF, and DMF) with different epoxy resin (SU-8 here) dissolving/swelling capacity are detected for the proof-of-principle demonstration. VOC solvents are gradually added to the water to obtain a serious of hybrid samples for the fluorescence sensing. The microstructures are placed in the hybrid solutions and their fluorescence spectra are recorded using the home-made micro-measuring system. Prior to the sensing assay, it is verified that the micro-structures' photo-bleaching is well controlled during optimized fluorescent sensing operation (i.e., fluorescent spectroscopic detection with properly short time and UV intensity). The micro-structures are exposed to UV light for up to 30 min with the same setups for sensing tests (~0.2 mW/cm^2), and the corresponding fluorescent spectra and images are recorded every 15 min. In Figure S17, after a consecutive 30 min exposure to UV irradiation, all the AIEoxe/SU-8 micro-structures maintain high-intensity fluorescence with no obvious photobleaching compared with the original state (over 90% fluorescent intensity remained). The fluorescence intensity ratio of b+r+gAIEoxes/SU-8 microcubes (I_{500}/I_{600}) almost remains unchanged after 30 min irradiation.

Waveguide measurement: In the waveguide measurement, a 405-nm exciting laser is focused at different positions along the wire of microwire. The excited green fluorescence is well confined and propagated along the microwire, and output at the two ends. And the output fluorescent intensity increases as the exciting spot gradually gets closer to the right tip. Both the PL intensities at illuminating spots (I_{body}) and emitting tips (I_{tip}) are recorded, and their ratio I_{tip}/I_{body} presents a single-exponential decay against the propagation distance. The optical loss coefficient (R) can be obtained by single-exponential fitting $I_{tip}/I_{body} = A \cdot \exp(-RD)$, in which D is the propagation distance between exciting spot and emitting tip.

Figure

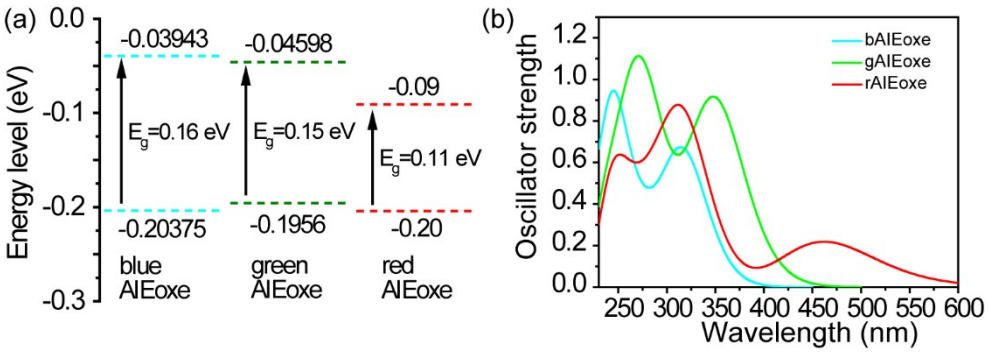

Figure S1. (a) Computed energy gaps and (b) predicted absorbance spectra for three AIEoxe molecules as calculated by TD-DFT method using B3LYP with the 6-31G(d) basis set.

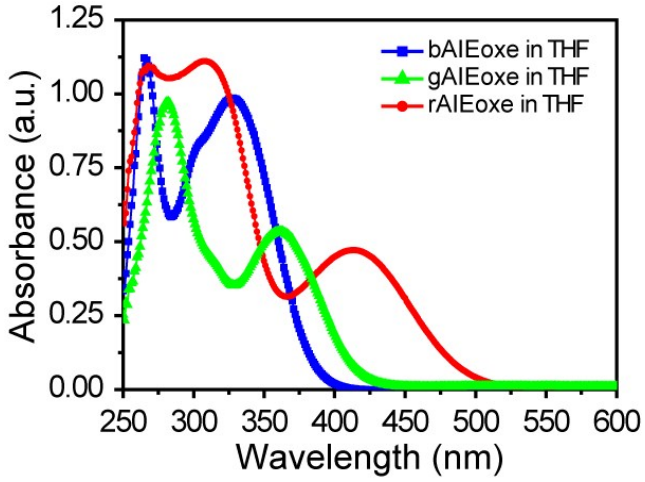

Figure S2. Experimentally measured Uv-vis absorption spectra for three AIEoxe molecules in the THF solution.

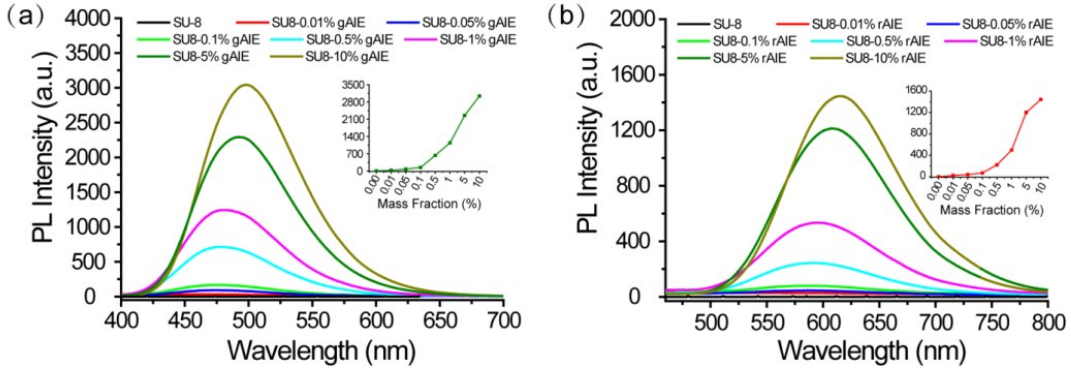

Figure S3. Fluorescence spectra of gAIEoxe and rAIEoxe in SU8 matrix with various doping concentrations. The insets are fluorescent intensity variation against different doping concentrations.

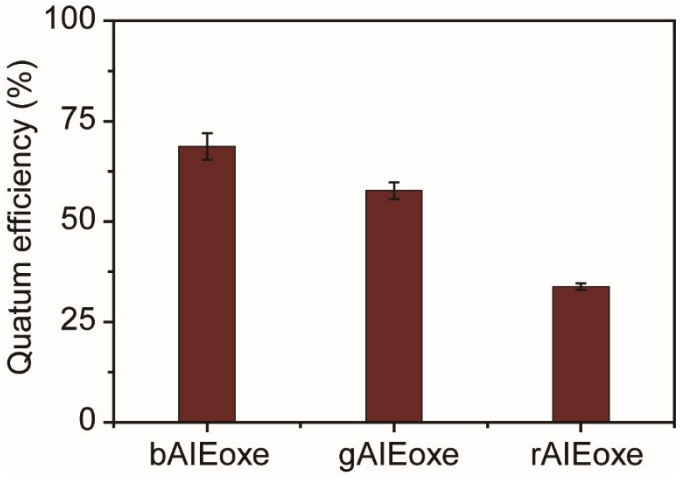

Fig. S4 The quantum efficiency of three AIEoxe molecules in the SU-8 matrix.

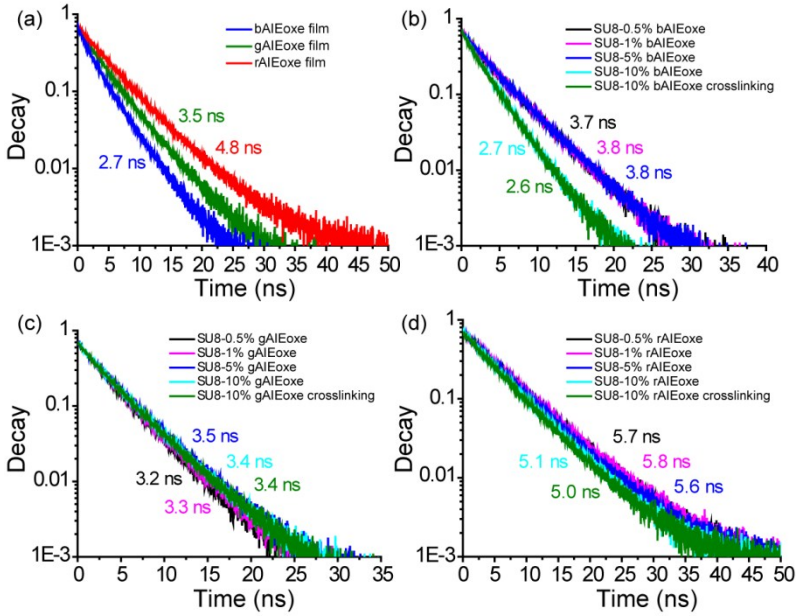

Figure S5. (a) Fluorescence lifetime of pure AIEoxe films. Fluorescence lifetime of SU8 composite films with different doping fraction of bAIEoxe (b), gAIEoxe (c) and rAIEoxe (d).

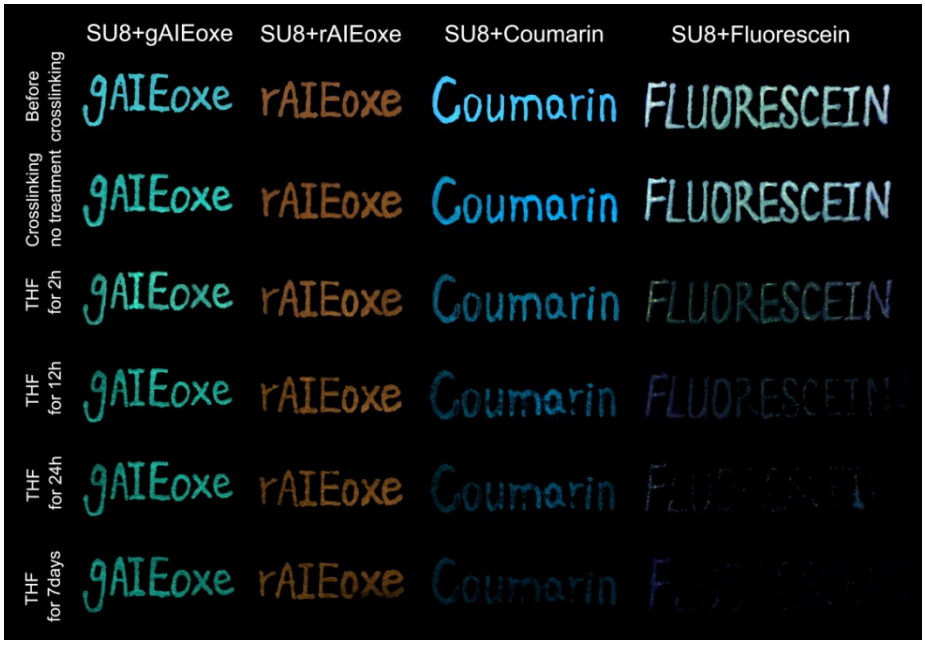

Figure S6. Chemical stability of the crosslinked handwritten patterns containing gAIEoxe, rAIEoxe, coumarin, and fluorescein molecules against THF treatment.

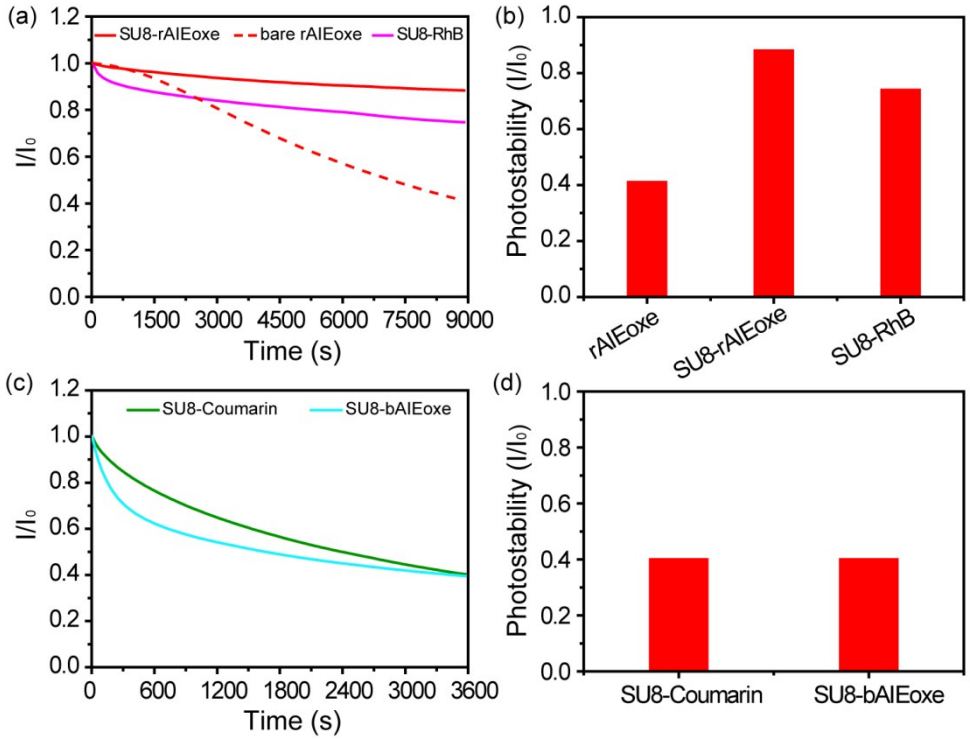

Figure S7. (a) Stability against photobleaching of SU8-rAIEoxe, SU8-RhB and bare rAIEoxe films under continuous illumination of a 150 W Xe-lamp for 2.5h. (b) the remaining fluorescence intensity of luminous dyes in (a) after 2.5h irradiation in comparison with their initial intensity. (c) Stability against photobleaching of SU8-bAIEoxe and SU8-Coumarin composite films under continuous illumination of a 150

W Xe-lamp for 1h. (d) the remaining fluorescence intensity of luminous dyes in (c) after 1h irradiation in comparison with their initial intensity.

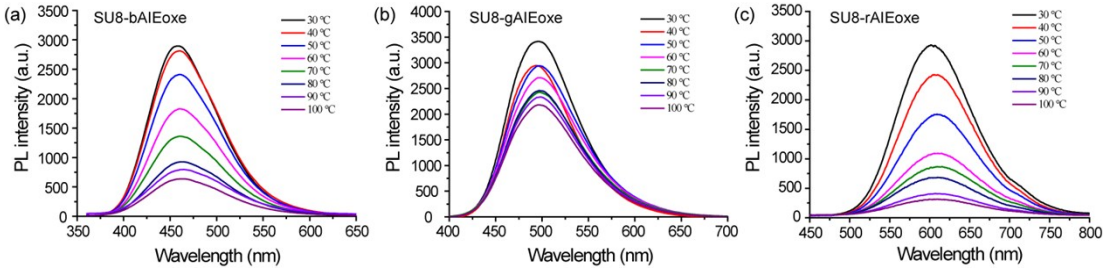

Figure S8. Fluorescence emission spectra of SU8-bAIEoxe (a), SU8-gAIEoxe (b) and SU8-rAIEoxe (c) under thermal treatment of different temperatures from 30°C to 100°C.

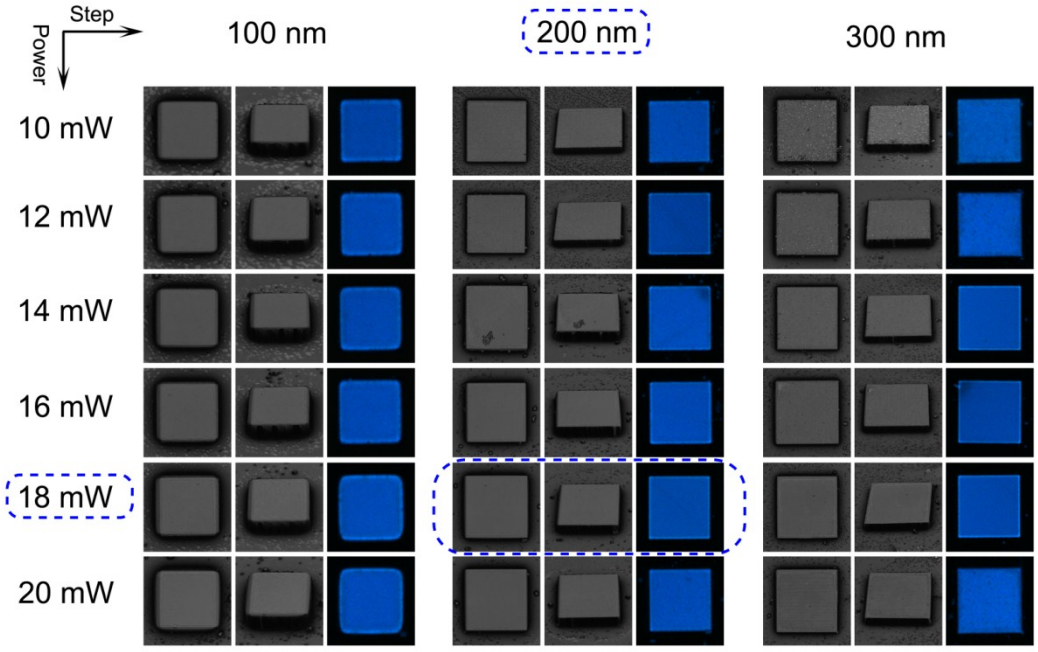

Figure S9. Optimization of FsLDW-processing parameters of bAIEoxe doped SU8 resin**.** Laser power intensity ranges from about 10 to 20 mW cm^{-2} and scanning step from 100 nm to 300 nm. The optimal parameter used for fabrication here is 18 mW cm^{-2} (laser power intensity), 200 nm (scanning step) and 200 μs (exposure time on single point). The size of micro-cube is 20×20 μm.

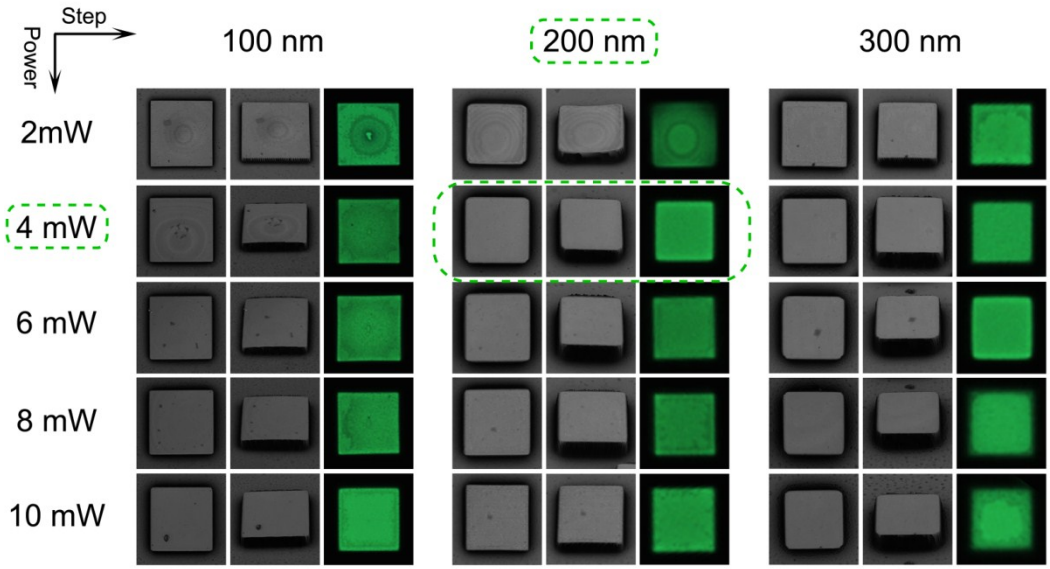

Figure S10. Optimization of FsLDW-processing parameters of gAIEoxe doped SU8 resin**.** Laser power intensity ranges from about 2 to 10 mW cm^{-2} and scanning step from 100 nm to 300 nm. The optimal parameter used for fabrication here is 4 mW cm^{-2} (laser power intensity), 200 nm (scanning step) and 200 μs (exposure time on single point). The size of micro-cube is 20×20 μm.

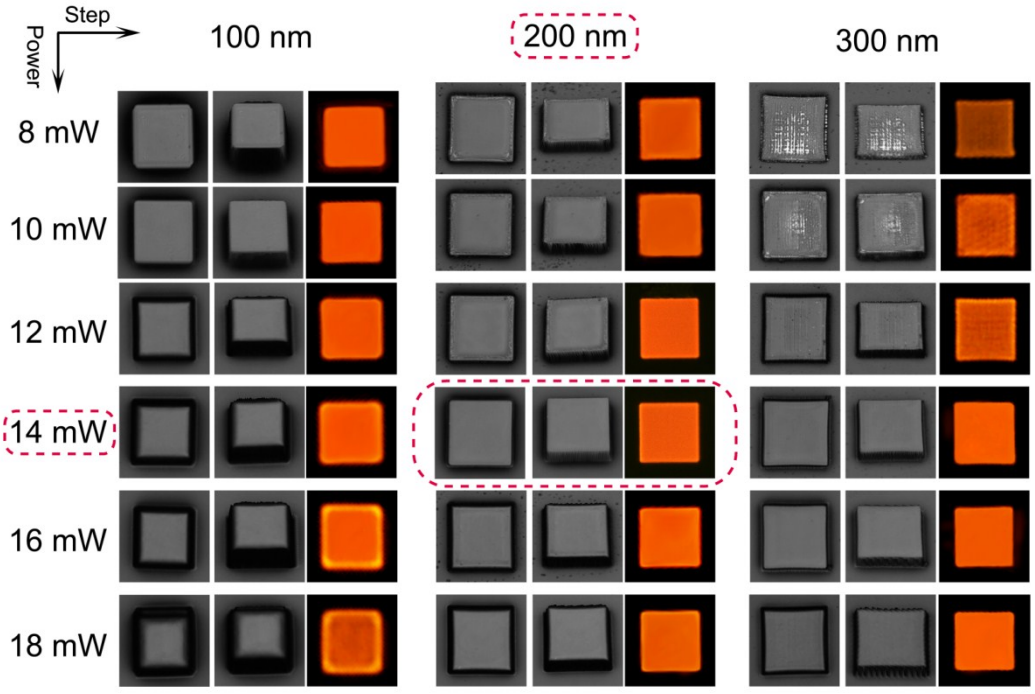

Figure S11. Optimization of FsLDW-processing parameters of rAIEoxe doped SU8 resin**.** Laser power intensity ranges from about 8 to 18 mW cm^{-2} and scanning step from 100 nm to 300 nm. The optimal parameter used for fabrication here is 14 mW cm^{-2}

(laser power intensity), 200 nm (scanning step) and 200 μs (exposure time on single point). The size of micro-cube is 20×20 μm.

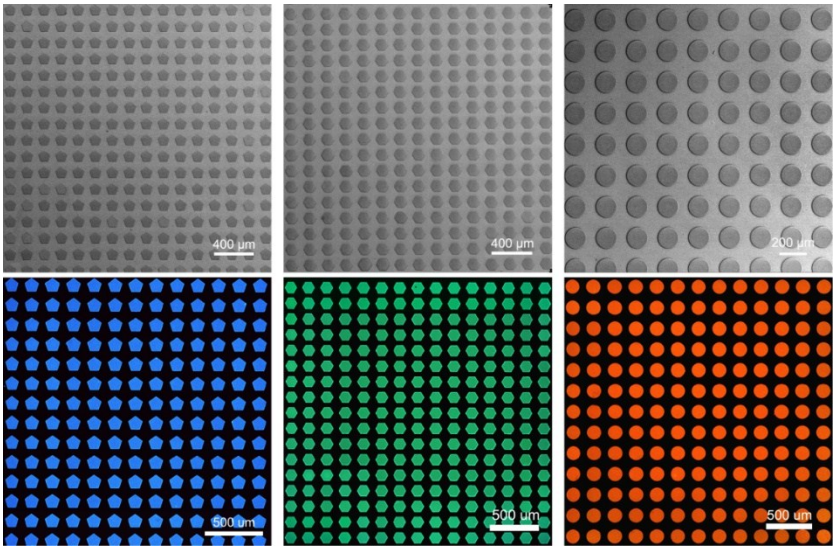

Figure S12. SEM and fluorescence microscope images of large-area SU8-AIEoxe micro-arrays fabricated by UV photolithography technique.

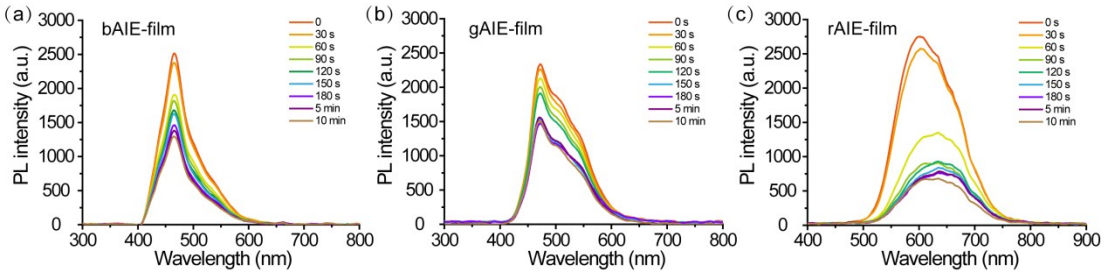

Figure S13. Fluorescent emission spectra of SU8 film incorporated with 10 wt % (a) bAIEoxe (b) gAIEoxe and (c) rAIEoxe against response time with exposure to saturated THF vapor.

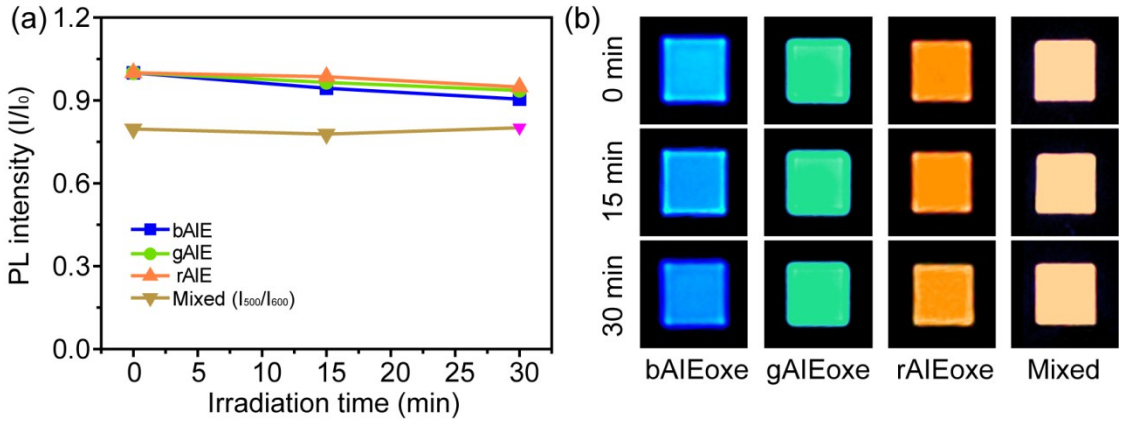

Figure S14. The photobleaching assay of different microcubes during the VOC sensing assay. (a) The fluorescence intensity change of mono-chromatic microcubes and the intensity ratio (I_{500}/I_{600}) change of multi-color microcubes with the irradiation of UV light for 1h. (b) the recorded fluorescent images (every 15 min) during the photobleaching assay.

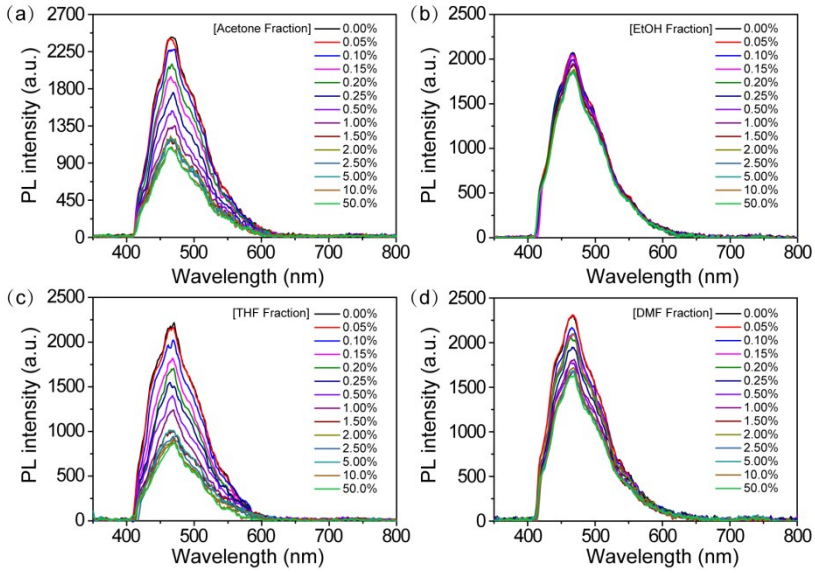

Figure S15. Fluorescent emission spectra of fabricated bAIEoxe micro-cubes under the treatment of aqueous solution with different amount of (a) Acetone, (b) EtOH, (c) THF and (d) DMF.

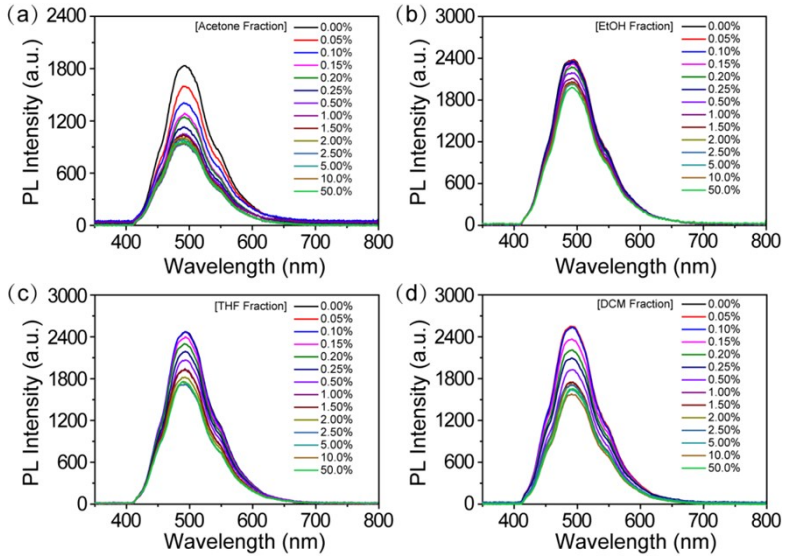

Figure S16. Fluorescent emission spectra of fabricated gAIEoxe micro-cubes under the treatment of aqueous solution with different amount of (a) Acetone, (b) EtOH, (c) THF and (d) DMF.

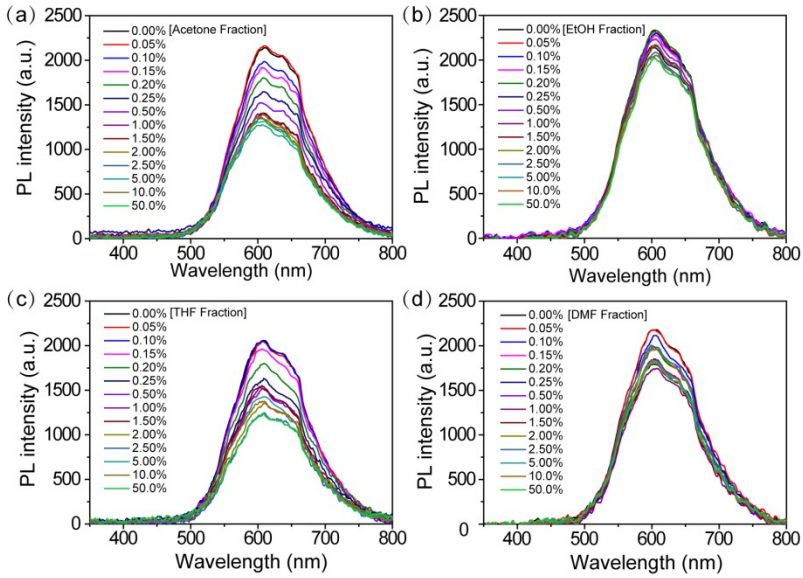

Figure S17. Fluorescent emission spectra of fabricated rAIEoxe micro-cubes under the treatment of aqueous solution with different amount of (a) acetone, (b) EtOH, (c) THF and (d) DMF.

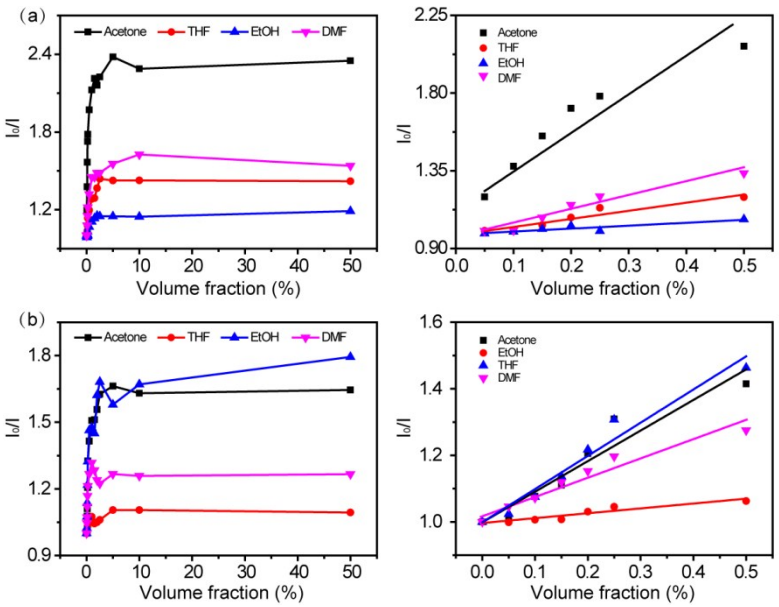

Figure S18. Relative fluorescence intensity change of micro-cubes containing (a) gAIEoxe and (b) rAIEoxe after treatment with the aqueous solution containing different content of acetone, THF, EtOH and DMF solvents. The left column is the overall change of fluorescence intensity in response of various VOC solutions ranging from 0% to 50% v/v while the right column is the detailed plot within 0.5% v/v.

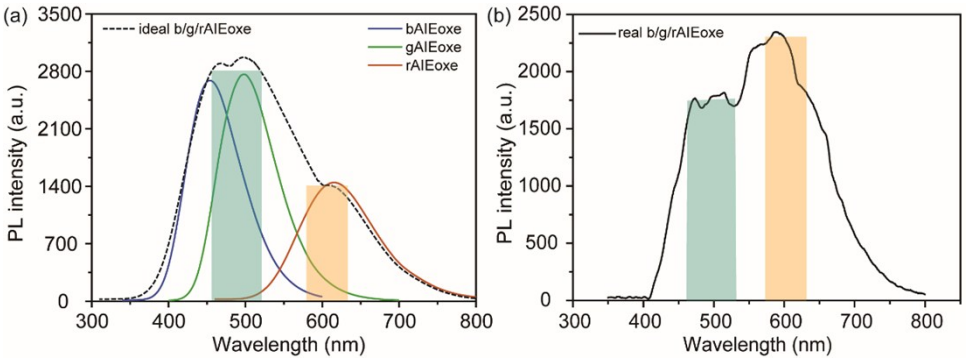

Figure S19. The emission spectrum of three monochromatic SU-8/AIEoxe and the ideal emission spectrum of fluoro-chromatic one without energy transfer. (b) The measured emission spectrum of three-color fluores-chromatic composite.

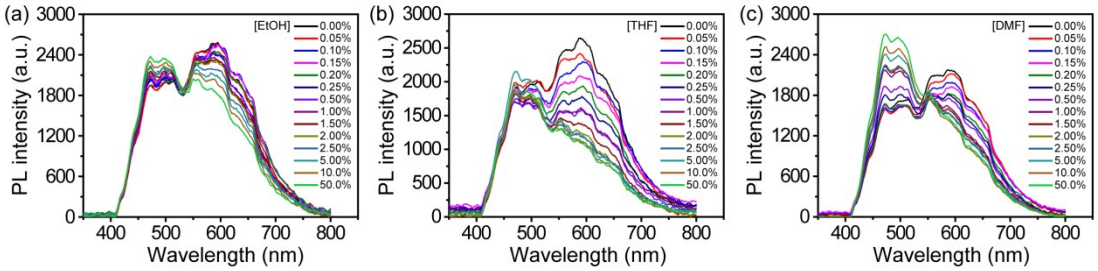

Figure S20. Fluorescent emission spectra of fabricated micro-cubes (20-μm) containing three AIEoxe dyes under the treatment of aqueous solution with different amount of (a) EtOH, (b) THF and (c) DMF.

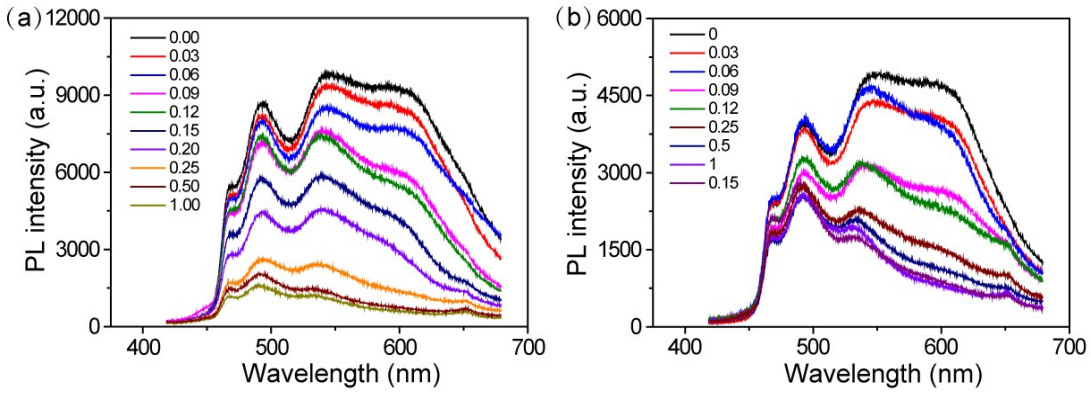

Figure S21. The spectral change of three-color mixed microwires (1-μm) in front of (a) DMF and (b) THF at different concentrations.

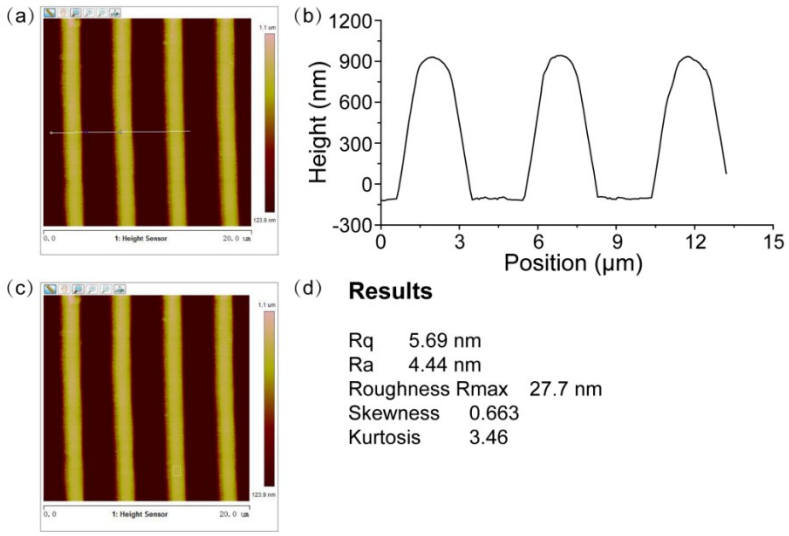

Figure S22. The cross section curve and roughness of the fabricated microwire characterized by AFM.

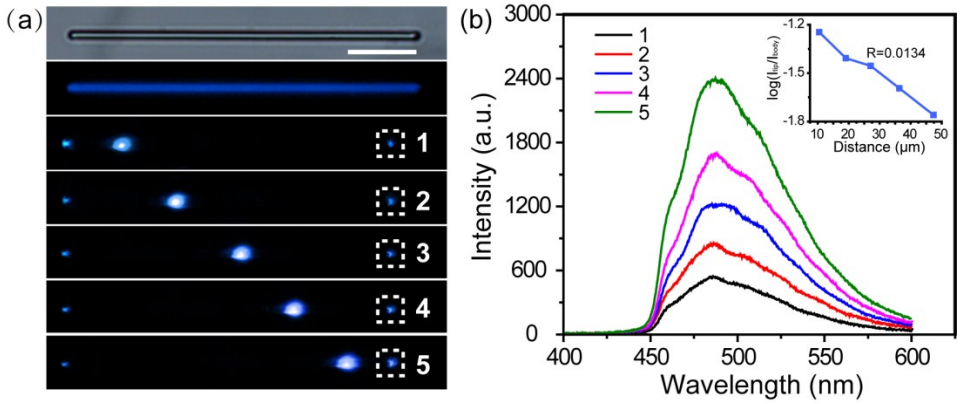

Figure S23. (a) Bright-field and fluorescence micrograph images of a bAIEoxe doped microwire by exciting different positions with a laser beam (400 nm). The scale bar is 10 μm. (b) Spatially resolved PL spectra recorded from the right tip of microwire with different propagation distances between the excitation spot and right tip of the microwire shown in (a). Inset: the relation of $\log(I_{tip}/I_{body})$ against propagation distance. The plot is linear fitted to obtain the optical loss coefficient R.

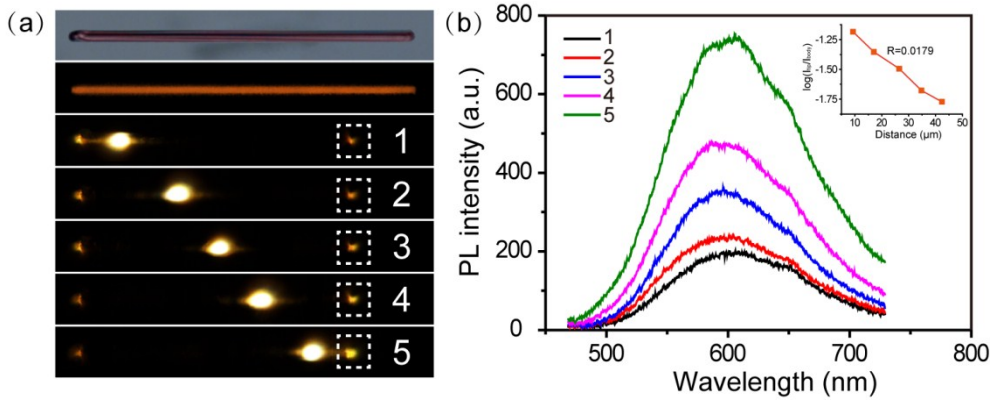

Figure S24. (a) Bright-field and fluorescence micrograph images of a rAIEoxe doped microwire by exciting different positions with a laser beam (400 nm). The scale bar is 10 μm. (b) Spatially resolved PL spectra recorded from the right tip of microwire with different propagation distances between the excitation spot and right tip of the microwire shown in (a). Inset: the relation of $\log(I_{tip}/I_{body})$ against propagation distance. The plot is linear fitted to obtain the optical loss coefficient R.

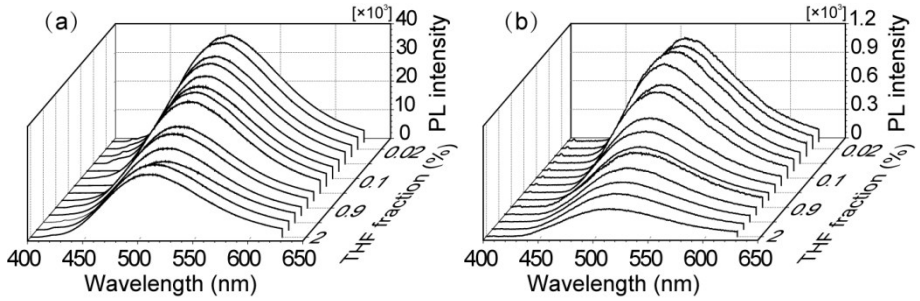

Figure S25. Fluorescence emission spectra of microwire at (a) the exciting spot and (b) the output side against the various THF content in water.

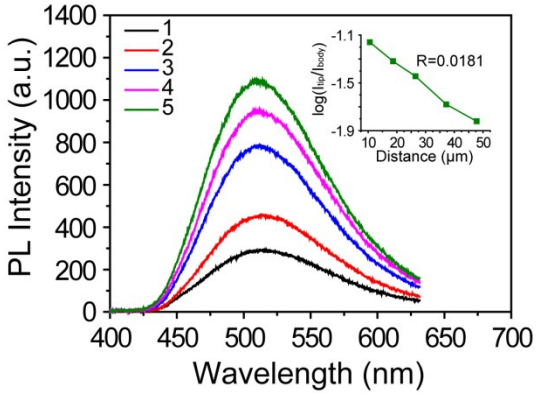

Figure S26. Spatially resolved PL spectra recorded from the right tip of gAIEoxe microwire with different propagation distances after the treatment of 2% THF aqueous solution for 10 min. Inset: the relation of $\log(I_{tip}/I_{body})$ against propagation distance. The plot is linear fitted to obtain the optical loss coefficient R.

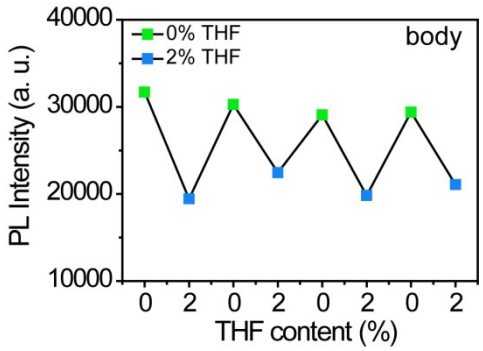

Figure S27. Reversible measurement of microwire's fluorescence intensity at the exciting sopt when exposed to THF aqueous solution (2%) and heat treatment at 90°C for 15 min (0%).

Table S1. The sensing parameters of AIEoxe composite microstructures with regard to different organic solvents in water.

		Acetone	THF	EtOH	DMF
bAIEoxe	Quenching ratio[a]	0.571	0.606	0.121	0.302
	Quenching contant (K_{sv})[b]	83.1	138.0	4.8	50.7
	LOD[c]	0.029%	0.015%	0.184%	0.031%
gAIEoxe	Quenching ratio	0.574	0.296	0.170	0.350
	Quenching contant (K_{sv})	207.4	60.7	20.9	116.8
	LOD	0.015%	0.061%	0.117%	0.038%
rAIEoxe	Quenching ratio	0.392	0.443	0.086	0.210
	Quenching contant (K_{sv})	65.2	62.7	14.2	31.5
	LOD	0.031%	0.028%	0.195%	0.052%
Mixed	LOD[d]	0.0124%	0.0232%	0.0782%	0.0133%
Microwire (gAIEoxe)	LOD (body)	-	0.0086%	-	-
	LOD (output)	-	0.004%	-	-
Microwire (Mixed)	LOD (body)	-	0.0033%	-	0.0019%
	LOD (output)	-	0.0072%	-	0.006%

[a]Quencing ratio represents relative PL intensity ratio ($1-I/I_0$) change after the treatment of VOC mixed aqueous solutions. [b]Quenching contant is calculated based on the Stern-Volmer relationship $I_0/I=1+K_{sv}[Q]$, in which I_0 and I are fluorescence intensity in the absence and presence of organic solvents, [Q] is the concentration of organic solvent in water, and K_{sv} refers to the Stern-Volmer constant. [c]The detection limit (LOD) of is estimated according to the equation LOD=3SD/|K|, where SD is the standard deviation of waveguide sample in blank solution (water) for 10 repeated detections, and K is the slope of PL intensity ratio of single emission versus VOC faction in water. [d]The detection limit (LOD) of is estimated according to the equation LOD=3SD/|K|, where SD is the standard deviation of emission ratio in blank solution (water) for 10 repeated detections, and K is the slope of PL intensity ratio (I_{500}/I_{600}) versus VOC faction in water.